Pharmacological Research 179 (2022) 106206

Contents lists available at ScienceDirect

Pharmacological Research

journal homepage: www.elsevier.com/locate/yphrs

# IL-3 signalling in the tumour microenvironment shapes the immune response *via* tumour endothelial cell-derived extracellular vesicles

Tatiana Lopatina [a,1], Malvina Koni [a,1], Cristina Grange [a,1], Massimo Cedrino [b], Saveria Femminò [a], Giusy Lombardo [a], Enrica Favaro [a], Maria Felice Brizzi [a,*]

[a] Department of Medical Sciences, University of Turin, Turin, Italy
[b] 2i3T Scarl University of Turin, Italy

ARTICLE INFO

*Keywords:*
Extracellular vesicles
IL-3
Tumour microenvironment
PD-L1
Tumour endothelial cells
Tumour immune editing

ABSTRACT

Antibody-based anti-cancer therapy is considered a successful approach to impair tumour progression. This study aimed to investigate the clinical impact of targeting the IL-3 signalling in the microenvironment of solid tumours. We intended to investigate whether the IL-3Rα blockade on tumour-derived endothelial cells (TEC) can modulate PD-L1 expression in tumour cells and peripheral blood mononuclear cells (PBMC) to reshape the anti-tumour immune response. Extracellular vesicles released by TEC after IL-3Rα blockade (aTEV) were used as the ultimate effectors of the antibody-based approach, while naive TEC-derived extracellular vesicles (nTEV) served as control. Firstly, we demonstrated that, either directly or indirectly *via* nTEV, IL-3 controls the expression of its receptor on TEC and PBMC respectively. Moreover, we found that nTEV, moulded by the autocrine secretion of IL-3, increased PD-L1 expression in myeloid cells both *in vitro* and *in vivo*. In addition, we found that nTEV-primed PBMC favour tumour cell growth (TEC and MDA-MB-231 cells), whereas PBMC-primed with aTEV still retain their anti-tumour properties. Isolated T-cells pre-conditioned with nTEV or aTEV and co-cultured with TEC or MDA-MB-231 cells have no effects, thereby sustaining the key role of myeloid cells in tumour immune editing. *In vivo* nTEV, but not aTEV, increased the expression of PD-L1 in primary tumours, lung and liver metastases. Finally, we demonstrated that the enrichment of miR-214 in aTEV impacts on PD-L1 expression *in vivo*. Overall, these data indicate that an approach based on IL-3Rα blockade in TEC rearranges EV cargo and may reshape the anti-tumour immune response.

## 1. Introduction

Tumour immune regulation leading to tumour tolerance is also orchestrated by tumour-derived extracellular vesicles (TEV) [1,2]. Extracellular vesicles (EV) are heterogenic membrane structures with a specific molecular composition dictated by their cell of origin. TEV have surface receptors and stimulating factors, such as, TLR4, HLA class I, HLA G, as well as inflammatory cytokines (TGFβ1, IFN, IL-6, IL-10) [2]. TEV are also enriched in immune relevant microRNA (miR-146, miR-214 and many others) [3–5].

TEV express tumour-associated antigens and neo-antigens conveyed by the parental tumour cells as well as major histocompatibility complex (MHC) class I and class II molecules [1]. Thus, TEV could present tumour antigens to antigen presenting cells and drive specific immune response [6]. The choice to trigger cytotoxic effect or immunosuppression depends on the presence of co-stimulatory factors. Indeed, it has been extensively reported that TEV promote tumour immune escape through different mechanisms [1,2]. This implies that, since TEV regulate the immune response, by facilitating communication between immune cells and cancer cells, they also impact on tumour progression and metastasis formation.

The programmed cell death-1 receptor (PD-1) is an immune checkpoint inhibitor, expressed on the surface of immune effector cells [7]. PD-1 is mainly activated by the programmed cell death ligand 1 (PD-L1), expressed by several cell types [8]. The PD-1/PD-L1 pathway fine-tunes inflammation also supporting tolerance of circulating T-lymphocyte [8]. In cancer, the expression of PD-L1 is recognized as one of the major immune escape mechanisms [7,9]. Indeed, in several cancers, PD-L1 is highly expressed and the PD-L1/PD-1 signalling is engaged to evade the T-cell-mediated immune regulation [7]. Additionally, PD-L1 was found

* Correspondence to: Department of Medical Sciences, University of Turin, Corso Dogliotti 14, 10126 Turin, Italy.
*E-mail address:* mariafelice.brizzi@unito.it (M.F. Brizzi).
[1] TL, MK, and CG contributed equally

https://doi.org/10.1016/j.phrs.2022.106206
Received 24 January 2022; Received in revised form 25 March 2022; Accepted 31 March 2022
Available online 6 April 2022

in TEV, derived from melanoma [8], prostate cancer [11], glioblastoma [10], and leukaemia [13] and has been detected in blood samples of cancer patients [14]. Recent studies have suggested that EV isolated from the blood samples of cancer patients express PD-L1, and that EV PD-L1 content correlates with patient's pathological features [12,15,16].

Tumour endothelial cells (TEC) strictly control tumour development and metastasis formation by allowing nutrient and oxygen supply, immune cell entrance, and managing the escape of tumour cells to reach secondary sites [17,18]. TEC are unique and differ from normal endothelial cells in term of proliferation surface protein expression, secretome, and released EV [19,20]. Moreover, naive EV released by TEC (nTEV) share with TEV several activities: the ability to promote vessel formation, the capability to restrain of the immune surveillance, and the enhancement of tumour growth and metastasis formation [2,4]. We have previously shown that TEC also express the receptor for interleukin 3 (IL-3Rα) [21]. More recently we provided evidence that the IL-3Rα blockade on TEC changes the content of their released EV (aTEV), impairing their oncogenic action [3,4]. Due to its highly expression in leukemic cells the impact of the IL-3Rα blockade has been extensively investigated in leukaemia patients [22], while poorly explored in solid tumours. Since nTEV suppress the immune response [2,6], while the impairment of IL-3 signalling in TEC, by the receptor blockade, interferes with tumour progression, we aimed to evaluate whether and how aTEV can also revert the immunosuppressive functions of nTEV in solid tumours. Particular attention has been devoted to investigate the impact of nTEV and aTEV in the regulation of PD-L1 expression.

## 2. Materials and methods

### 2.1. nTEV and aTEV isolation

TEC were isolated as previously described [23] and grown in the complete EndoGro medium (Millipore) supplemented with 2% of fetal bovine serum (FBS). TEC were functionally evaluated to form vessel-like structures at different passages. The expression of IL-3Rα on TEC untreated or stimulated with IL-3 was evaluated by Fluorescence-activated cell sorting (FACS) using anti-human IL-3Rα antibody (Miltenyi Biotec, #130–113–322).

For nTEV isolation, confluent TEC were cultured in serum-free DMEM for 18 h. For aTEV collection, TEC were treated with 1 μg/ml of anti-human IL-3Rα mouse antibody (R&D Systems, #MAB301–100, Clone 32703) in serum-free DMEM. The conditioned medium from TEC untreated or treated with the blocking IL-3Rα antibody was centrifuged for 30 min at 3.000 g to remove cell debris and apoptotic bodies. Then the supernatant was filtered with PES membrane filters (0.22 μm, Millipore) and submitted to ultracentrifugation for 2 h at 100.000 g at 4 °C, using the Beckman Coulter Optima L-100 K Ultracentrifuge with the rotor type 45 Ti 45000RPM. The EV pellets were resuspended in DMEM supplemented with 1% of DMSO and stored at − 80 °C until further use. After thawed, EV aliquots were resuspended in PBS and analysed using the Nanoparticle tracking analysis (NTA) by NanoSight NS300 system (Malvern Instruments, Ltd) and transmission electron microscopy (Jeol JEM 1400 Flash electron microscope, Jeol, Tokyo, Japan) [24]. For further characterisation ExoView analysis (NanoView Biosciences), and MACSPlex exosome kit (Miltenyi Biotech) were used according to manufacturer instructions.

Western blot analysis for nTEV and aTEV was performed using 7% sodium dodecyl sulfate–polyacrylamide gel electrophoresis. Immunoblotting with anti-human CD63 (Abcam, #ab134045), CD81 (Abcam, #ab109201), CD9 (Abcam, #ab223052), CD29 (Invitrogen, #Ma5–17103), and GM-130 (Abcam, #ab52649) antibody was performed overnight at 4 °C. Appropriate secondary HRP-labelled anti rabbit or mouse antibody (BioRad) were used at 1:1000 dilution for 1 h at room temperature. The protein bands were visualized with chemiluminescence (ECL) detection kit and ChemiDoc™ XRS + System (BioRad). Lysates from cells, nTEV, and aTEV were loaded at concentration of 10 μg/well.

### 2.2. PBMC isolation and treatment with nTEV or aTEV

Fresh human PBMC were isolated by density gradient (Ficoll, Sigma) centrifugation from heparinized blood samples obtained from healthy donors. The use of PBMC was approved by the Ethic Committee of A.O. U. Città della Salute e della Scienza di Torino, Turin, Italy (CS2/1255–Protocol number 0050416, May 16, 2019). PBMC were seeded in 6-well plates at the density of $2 \times 10^7$/well in 2 ml of serum-free AIM V medium. nTEV or aTEV were added to PBMC at the concentration of $1 \times 10^{10}$/ml (approximately $1 \times 10^3$ EV/cell) for at least 24 h. As control, we used non-stimulated PBMC. After 24 h or 5 days, PBMC were counted using Muse® Count & Viability Kit (Luminex), analysed by FACS using the anti-human IL-3Rα antibody (#306014, Biolegend), or used for co-culture experiments or for T-cell isolation. In selected experiments, T-cells were isolated from fresh PBMC (naive) seeded at the density of $1 \times 10^7$/well in 2 ml of serum-free AIM V medium and stimulated as indicated.

For PD-L1 analysis, approximately $1 \times 10^6$ PBMC, cultured for 48 h in the presence of nTEV or aTEV were resuspended in 100 μl of PBS supplemented with 0.1% bovine serum albumin and incubated with anti-human PD-L1 antibody (Miltenyi Biotec, #130–122–809) or PE non-immune isotypic IgG for 30 min at 4 °C. Then the cells were washed and analysed using CytoFlex from Beckman Coulter.

T-cells were isolated before or after preconditioning PBMC with nTEV or aTEV using Dynabeads™ Untouched™ Human kit (Invitrogen, #11344D) according to the manufacturer instructions.

### 2.3. ELISA assay

Relative quantification of IL-1β, IL-10, and TGFβ1 secretion by PBMC pre-treated with nTEV or aTEV alone or co-cultured with tumour cells (MDA-MB-231 and TEC) was performed using DuoSet ELISA Development Systems (R&D Systems) according to manufacturer instructions. Naive PBMC served as internal control.

### 2.4. Co-culture of PBMC and TEC or MDA-MB-231 cells

To study the expression of the IL-3Rα on TEC, 0.4 μm pore transwells (Costar, #3412) were used for co-culture experiments with PBMC pre-treated with nTEV or aTEV. $1 \times 10^5$ TEC were seeded in 6-well plates and PBMC were stimulated with nTEV or aTEV as above described. After 24 h pre-stimulated PBMC were plated in the upper chamber of the transwell at the concentration of $5 \times 10^6$/well and put onto TEC. After additional 48 h TEC were analysed by FACS using the anti-human IL-3Rα antibody (Miltenyi Biotec, #130–113–322).

To evaluate the cytotoxic effects of PMBC against tumour, a direct cell-to-cell contact cultures were used. To this end, freshly isolated PBMC were stimulated with nTEV or aTEV as above described for 24 h, meanwhile TEC or MDA-MB-231 cells were labelled with CFSE and seeded in 6-well plates, at the concentration of $1 \times 10^5$/well. The day after, $5 \times 10^6$ of pre-stimulated PBMC were plated on TEC or MDA-MB-231 cells for 48 h. As control, we used TEC or MDA-MB-231 cells cultured alone or co-cultured with untreated PBMC. Six independent experiments were performed in duplicates.

### 2.5. Tumour in vivo models

Animal studies were conducted in accordance with the Italian National Institute of Health Guide for the Care and Use of Laboratory Animals (protocol No. 833/2020-PR). Mice were housed according to the guidelines of the Federation of European Laboratory Animal Science Association and the Ethical Committee of the University of Turin. The investigators (at least 2) were blinded when assessing the outcome. To

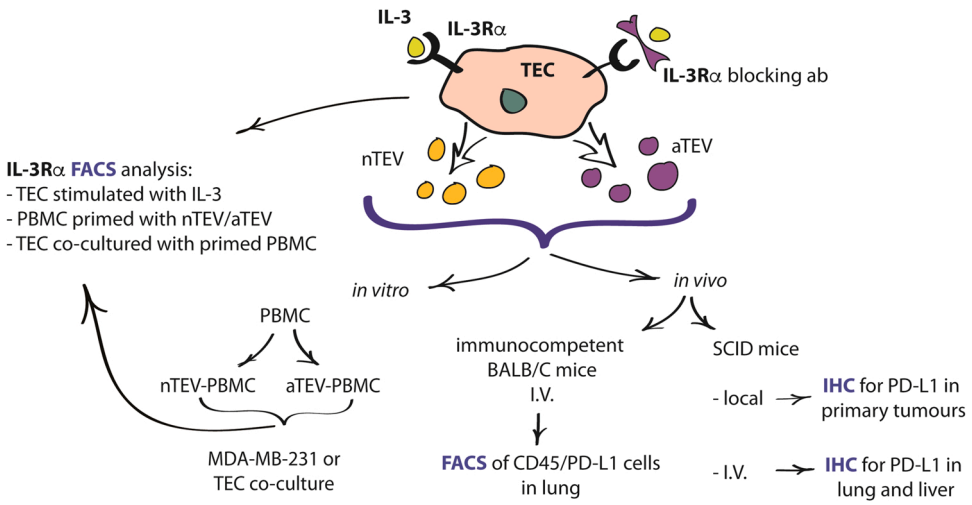


**Fig. 1.** Scheme of the *in vitro* and *in vivo* studies. FACS or IHC were used for PD-L1 detection. FACS analysis for IL-3Rα expression. I.V.: intravenously; IHC: immunohistochemistry.

investigate nTEV- or aTEV-mediated immune regulation *in vivo,* we used the immunocompetent female BALB/C mice. We treated mice intravenously (I.V.) with nTEV or aTEV ($1 \times 10^{10}$/injection) 5 times during 2 weeks. The day after the last nTEV or aTEV injection, mice were sacrificed and PD-L1 was analysed in different tissues by FACS. To this end, the tissues were homogenized and cells positive for mouse PD-L1 (Biolegend, #124334) and CD45 (Miltenyi Biotec, #130–110–798) were detected.

Primary tumours were obtained by injecting subcutaneously Matrigel containing TEC in SCID mice (8 weeks/female) (4 mice/group) ($1 \times 10^6$ cells/injection). Matrigel plugs containing TEC were locally injected with saline, nTEV, or aTEV ($1 \times 10^{10}$/plug) at the third and seventh day after implantation. At day 10, the recovered plugs were embedded in paraffin (n = 4/each condition) and PD-L1 expression was analysed by immunohistochemistry, using the anti-human rabbit PD-L1 antibody (Abcam, #ab233482).

For the metastasis model, SCID mice were pre-treated intravenously with nTEV or aTEV for 5 days ($1 \times 10^{10}$/injection). On day 5, $0.6 \times 10^6$ MDA-MB-231 cells were injected I.V. The mice were sacrificed after 5 weeks and lung and liver tissues analysed for PD-L1 expression. Liver metastases were also counted according to human PD-L1 expression.

### 2.6. Immunohistochemistry for PD-L1 detection in the lung and liver

Immunohistochemistry was performed using an automated slide-processing platform (Ventana BenchMark AutoStainer, Ventana Medical Systems), with Universal DAB Detection Kit detection systems. The anti-human PD-L1 rabbit polyclonal antibody (Abcam #ab233482) was diluted 1:100. Secondary HRP-labelled anti-rabbit antibody (Goat Anti-Rabbit IgG (H+L)-HRP Conjugate, BioRad) was used at 1:1000 dilution for 1 h at room temperature. Sections were counterstained with haematoxylin, dehydrated, and mounted. Quantification of the PD-L1 expression was performed using Fiji software (ImageJ). The results were expressed as mean ± SD of PD-L1 positive area (related units) per sample (10 images/section, 4 samples/each condition).

### 2.7. miR-214 enrichment in nTEV

To obtaining nTEV enriched in miR-214, TEC growing in 75 cm cultured flasks were transfected with HiPerfect reagent (Qiagen) using 20 μM hsa-miR-214 Pre-miR™ miRNA Precursor (PM12124, Invitrogen) according to manufacturer instructions. TEC transfected with scramble mimic were used as control. The day after transfection fresh FBS-free DMEM was replaced for additional 24 h and collected for nTEV_miR-214 or Scramble miRNA_TEV isolation. We used PCR to confirm the enrichment of miR-214 in nTEV_miR-214. Briefly, single-stranded cDNA was generated from total RNA sample (80 ng) by reverse transcription using miScript Reverse Transcription Kit (Qiagen) following the manufacturer's protocol. miR-214 content was measured by qRT-PCR using the miScript SYBR Green PCR Kit (all from Qiagen). All reactions were performed using an Applied Biosystems 7900HT real-time PCR instrument and run in triplicate (3 ng of cDNA for each reaction) as described by the manufacturer's protocol (Qiagen). Relative miR-214 expression was normalized to the mean expression value of RNU6 and actin housekeeping genes. Data were analysed using Expression Suite Software (ThermoFisher).

### 2.8. Statistical Analysis

All data are reported as mean ± SD. Comparison between two groups was analysed by Student's t-test. Data passed both normality and equal-variance tests. One-way ANOVA followed by Tukey's multiple-comparison test was used for comparison among 3 or more groups; $p$-value $< 0.05$ was considered as significant. All *in vitro* or *in vivo* data are representative of at least 4 independent experiments. Graph Pad Prism version 5.04 (Graph Pad Software) was used for all statistical analyses.

## 3. Results

### 3.1. nTEV and aTEV characterisation

Firstly, nTEV and aTEV were characterized (see the scheme of the study, Fig. 1). As shown by TEM and NanoSight (data not shown), nTEV and aTEV did not differ in size (Supplementary Fig. S1). ExoView (NanoView Biosciences), MACSPlex (Miltenyi Biotech), and Western blot analyses, revealed a similar pattern of surface marker expression (CD9, CD29, CD63, and CD81) (Supplementary Fig. S1). We failed to detect PD-L1 on both nTEV and aTEV (data not shown).

### 3.2. IL-3Rα expression in TEC

This study has been designed to investigate the potential "clinical" impact of targeting TEC using a blocking IL-3 receptor antibody, and, in particular, the effect on PD-L1 expression. Therefore, the expression of IL-3Rα was first evaluated on naive or IL-3 stimulated TEC. Moreover, since IL-3 is mostly released by activated T-cells [24], to mimic the TME, IL-3Rα was also analysed on TEC stimulated with nTEV-primed PBMC (Fig. 1). As shown by FACS analysis, IL-3 significantly up-regulated the

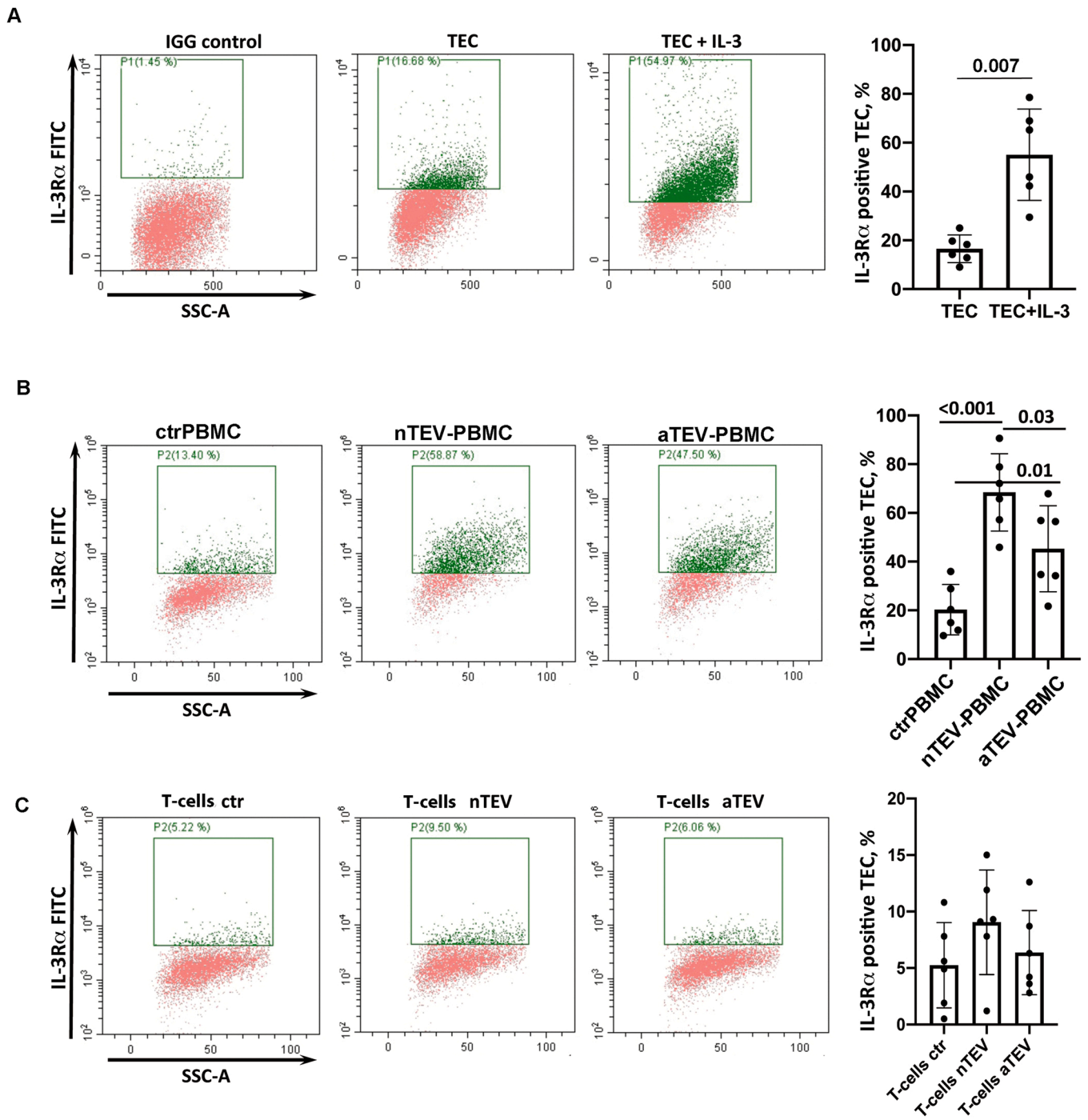


**Fig. 2.** IL-3Rα is up-regulated in TEC co-cultured with primed PBMC and T-cells, and stimulated with IL-3. (A) Representative FACS dot plots of untreated or IL-3 stimulated TEC (24 h). (B) Representative FACS dot plots of TEC co-cultured with control PBMC (ctrPBMC) or PBMC primed with nTEV or aTEV (24 h). (C) Representative FACS dot plots of TEC co-cultured with unstimulated T-cells or T-cells primed with nTEV or aTEV (24 h). Data are presented as the mean ± SD, n = 6.

expression of its receptor on TEC (Fig. 2A). No differences in PBMC viability at both 24 h and 5 days, as well as in IL-3Rα expression (24 h) upon nTEV and aTEV priming were detected (Supplementary Fig. S2A-B).

Then we evaluated the expression of IL-3Rα in TEC co-cultured with nTEV or aTEV-primed PBMC. We demonstrated that PBMC primed with nTEV, but not with aTEV, significantly increased the expression of the IL-3Rα (Fig. 2B). Interestingly, naive T-cells (isolated from naive PBMC) pre-treated with nTEV or aTEV failed to induce the expression of IL-3Rα on TEC (Fig. 2C), suggesting a key role of myeloid cells in the transfer of nTEV signals.

### 3.3. PBMC primed with aTEV retain their anti-tumour properties

TME immunosuppression also stems from EV-mediated communications [1]. Therefore, the effect of nTEV and aTEV in shaping PBMC anti-tumour action was further investigated. To this end, PBMC were pre-stimulated with nTEV or aTEV for 24 h, and the secretion of inflammatory factors was first analysed. We found that nTEV significantly enhance the secretion of IL-10 and TGFβ1, while aTEV increase the release of IL-1β (Fig. 3 A). We then investigated the impact of PBMC, either untreated or primed with nTEV or aTEV, in co-cultures (direct contact) with CSFE-labelled MDA-MB-231 cells or TEC for 48 h. As

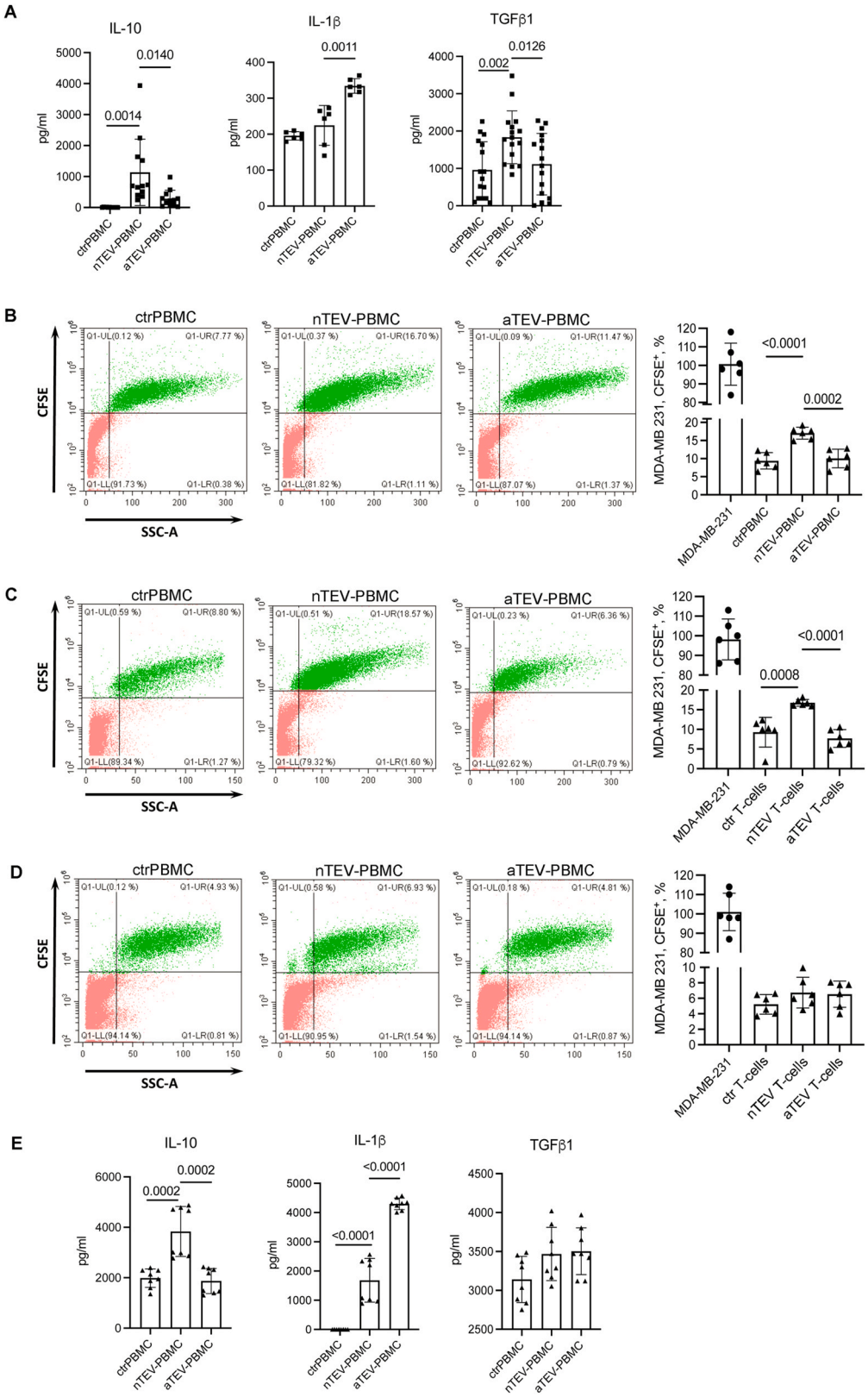


**Fig. 3.** nTEV, unlike aTEV, primed PBMC are impaired in their cytoxic activity. (A) Diagrams of IL-1β, IL-10, and TGFβ1 secretion by naive (ctrPBMC) or PBMC pre-treated with nTEV or aTEV. (B) Representative FACS dot plots of MDA-MB-231 cells co-cultured with ctrPBMC or PBMC pre-treated with nTEV or aTEV. Diagram represents data on MDA-MB-231 cells cultured alone (circles) or with the aforementioned PBMC (triangles). (C) Representative FACS dot plots and diagram of MDA-MB-231 cells co-cultured with T-cells, isolated from ctrPBMC or from PBMC pre-treated with nTEV or aTEV. (D) Representative FACS dot plots and diagram of MDA-MB-231 cells co-cultured with naive T-cells (isolated from ctrPBMC) pre-treated with nTEV or aTEV. (E) Diagrams of IL-1β, IL-10, and TGFβ1 secretion by ctrPBMC or PBMC pre-treated with nTEV or aTEV co-cultured with MDA-MB-231 cells. Diagram data are presented as the mean ± SD (at least n = 6 independent experiments).

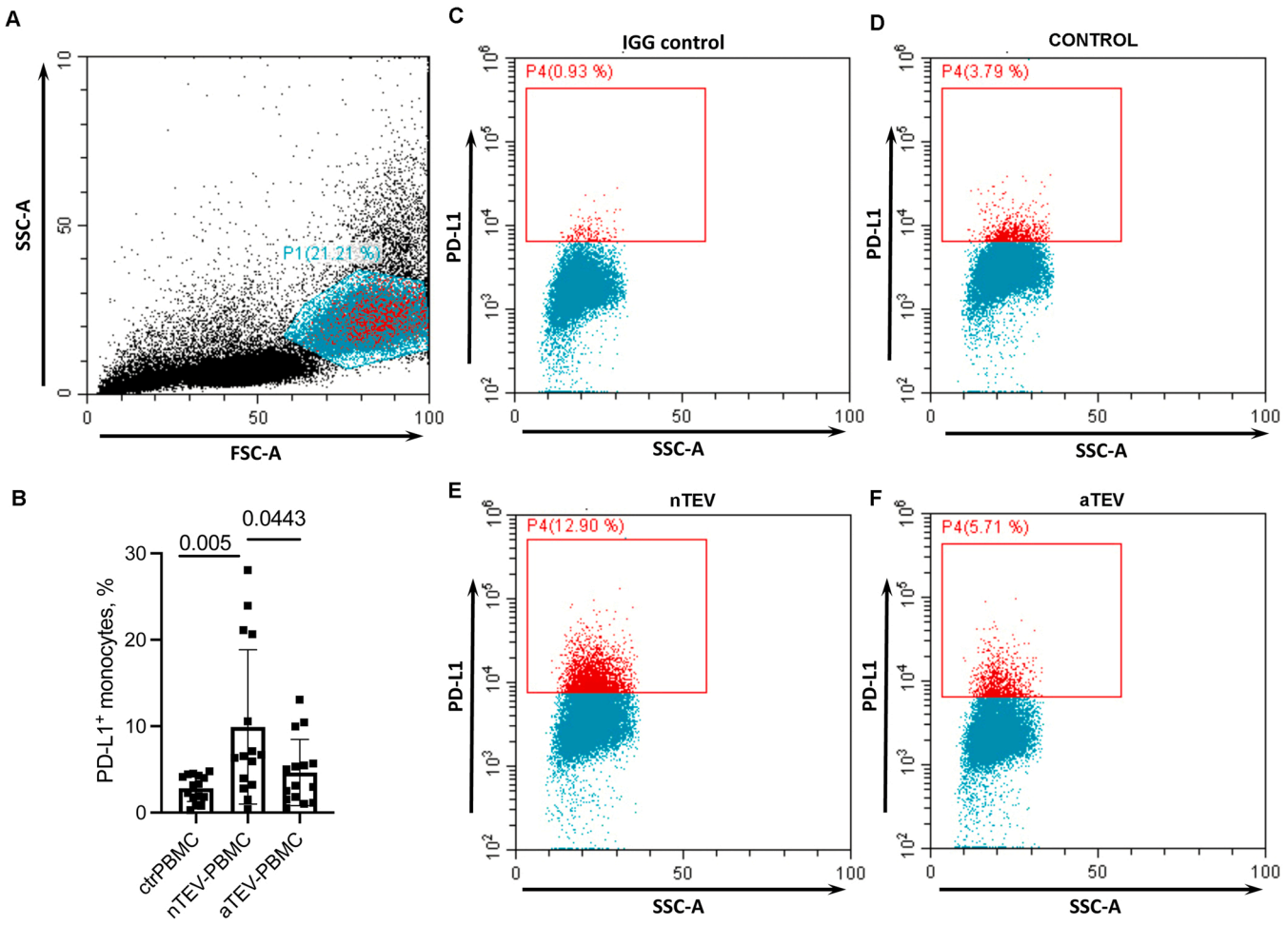


**Fig. 4.** nTEV, unlike aTEV, upregulated PD-L1 expression on PBMC. (A) Representative FACS dot plot image showing PBMC gating. (B) Diagram of PD-L1 expression on PBMC. Data are presented as the mean ± SD, n = 15 independent experiments. (C-F) Representative FACS dot plot images of ctrPBMC incubated with IGG control antibodies (C), ctrPBMC (D), nTEV primed PBMC (E), and aTEV primed PBMC (F) stained with anti-human PD-L1 PE conjugated antibody. In red are indicated PD-L1$^+$ cells.

shown in Fig. 3B and Supplementary Fig. S3A we demonstrated that, while the percentage of living cells decreases in the presence of PBMC, the cytotoxic activity of nTEV primed PBMC was reduced compared to both naive and aTEV primed PBMC. To investigate whether changes in PBMC secretome may contribute to the different immune response, ELISA assay was also performed on these conditioned media. The results reported in Fig. 3D and Supplementary Fig. S3E revealed that in the presence of nTEV primed PBMC IL-10 secretion was increased. Conversely, and consistent with functional data, a reduced secretion of IL-10 and an increased level of IL-1β were detected in co-cultures containing aTEV primed PBMC. Of note, the release of TGFβ1 did not change (Fig. 3E, Supplementary Fig. S3E). We also investigated the contribute of T-cells. The role of T-cells in mediating the cytotoxic effect was confirmed by the observation that T-cells isolated from aTEV-primed PBMC were still able to exert anti-tumour effect when seeded together with MDA-MB-231 cells (Fig. 3 C) and TEC (Supplementary Fig. S3B). Conversely, no effect was detected when naive T-cells primed with nTEV or aTEV were co-cultured with MDA-MB-231 cells and TEC (Fig. 3D, Supplementary Fig. S3C). These data indicate that nTEV contribute to suppress the immune response and myeloid cells are key supervisors.

### 3.4. aTEV fine-tune PD-L1 expression

To evaluate if the expression of PD-L1 in myeloid cells may contribute to our observations, FACS analysis was first performed on PBMC primed with nTEV or aTEV. We found that, unlike aTEV, nTEV significantly increased the expression of PD-L1 on myeloid cells (Fig. 4).

Since no data are so far available on the role played by nTEV and, most importantly, by aTEV in an immunocompetent context, *in vivo* experiments were performed in BALB/C mice intravenously injected with nTEV or aTEV for 2 weeks (Fig. 5 A). PD-L1 and CD45 co-expression were evaluated in lung, bone marrow, spleen, and peripheral blood by FACS analysis. As shown in Fig. 5B, the number of PD-L1$^+$/CD45$^+$ cells was significantly increased in the lung of nTEV-treated animals, but not in spleen, bone marrow, and peripheral blood (data not shown). Of note, we found that aTEV *in vivo* administration reduced the percentage of PD-L1$^+$/CD45$^+$ cells isolated from the lung.

Since tumour cells also express PD-L1 and contribute to immune evasion, the ability of nTEV and aTEV to regulate its expression on TEC derived tumours was further evaluated. We demonstrated that intratumour injection of nTEV in Matrigel plugs containing TEC enhanced PD-L1 expression, while aTEV significantly reduced its expression (Fig. 5 C,D). This indicates that nTEV and aTEV can control PDL-1 expression in different cell population in the TME, including, at least, myeloid cells and tumour cells.

Finally, to investigate the possibility that aTEV may also impact on tumour cell recruitment by regulating PD-L1 expression on homed cells, nTEV and aTEV were injected intravenously for 5 consecutive days before MDA-MB-231 cell administration (Fig. 6 A). The expression of

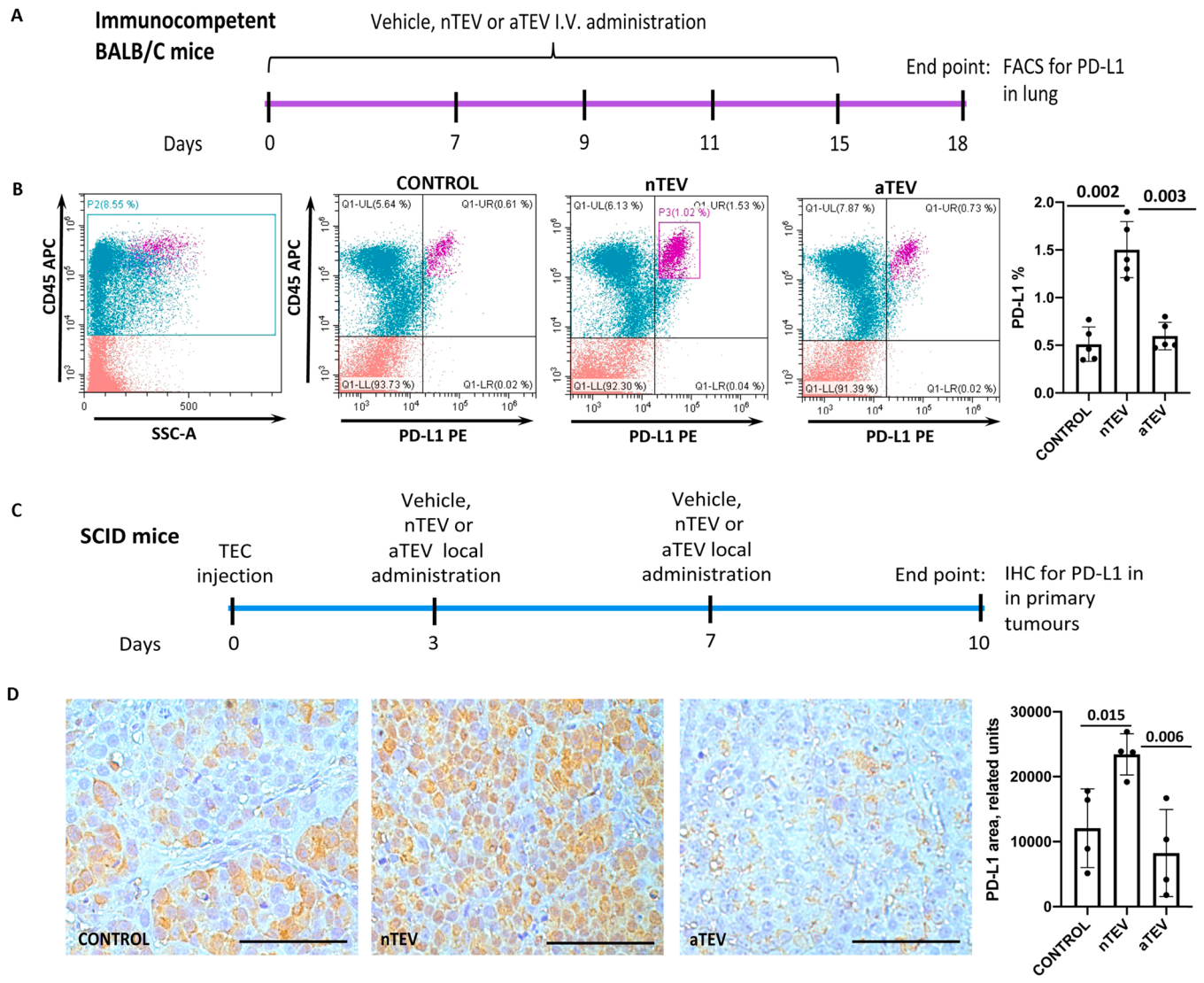


**Fig. 5.** nTEV, but not aTEV, increase the expression of PD-L1 in the lung and primary tumours. (A) Schematic representation of the *in vivo* study. (B) Representative FACS dot plot images showing $CD45^+/PD\text{-}L1^+$ lung-derived cells from control, nTEV, and aTEV treated mice. Data are presented as the mean ± SD, n = 5. (C) Schematic representation of the *in vivo* study in SCID mice. (D) Representative images of Matrigel containing TEC treated with nTEV, or aTEV stained with PD-L1 antibody. Saline treatment served as control. Scale bars = 100 μm (original magnification, 400X). Diagram data are presented as the mean ± SD, n = 4. I.V.: intravenously; IHC: immunohistochemistry.

PD-L1 was analysed in the lung and liver of immune-deficient animals. As shown in Fig. 6B-C, $PD\text{-}L1^+$ area were significantly increased in mice primed with nTEV both in the lung and liver tissues. Again, in aTEV treated animals a significant reduction of $PD\text{-}L1^+$ area was detected in both organs. Finally, as previously reported in the lung [4] a reduced number of metastatic foci was detected in the liver of aTEV primed animals (Fig. 6 C).

This observation provides evidence that aTEV priming can prevent the recruitment/homing of $PD\text{-}L1^+$ tumour cells both in the lung and in the liver. More importantly, these results indicate that disturbing the IL-3 signalling on TEC drives changes on their released aTEV, impacting on the expression of PD-L1 in both tumour and $CD45^+$ cells.

### 3.5. *miR-214 enrichment in aTEV regulates the expression of PD-L1*

We have previously shown that aTEV miRNA content is relevant for their biological action [3,4]. It has been shown that miR-214 post--transcriptionally regulate PD-L1 expression in B-cell lymphoma [25]. Since miR-214 was found enriched in aTEV [3], we south to determine whether miR-214 enrichment could also control PD-L1 expression in our model. To this end, the effect of nTEV enriched in miR-214 (nTEV_-miR-214) was evaluated *in vivo*. Matrigel plugs containing TEC were therefore locally injected with nTEV, aTEV, or nTEV_miR-214. Similarly to aTEV, nTEV_miR-214 treatment reduced the number of $PD\text{-}L1^+$ cells in TEC formed tumours (Fig. 7) compared to nTEV. These data further confirm the role of miR-214 in the regulation of PD-L1 expression [25].

## 4. Discussion

In the present study, we have shown that IL-3 signalling in TEC regulates the release of pro-metastatic nTEV that suppress the immune response by enhancing PD-L1 expression on tumour and myeloid cells. Conversely, an approach based on IL-3Rα blockade on TEC led to the release of aTEV enriched in miR-214 that retune the aberrant anti-tumour immune response reshuffling PD-L1 expression. Overall, these findings provide evidence that blocking IL-3 signalling in the TME amends PD-L1 expression and reshapes the anti-tumour immune response.

Blocking the interaction between PD-1 and PD-L1 became a revolution in cancer therapeutic approaches, particularly for lung, kidney, and

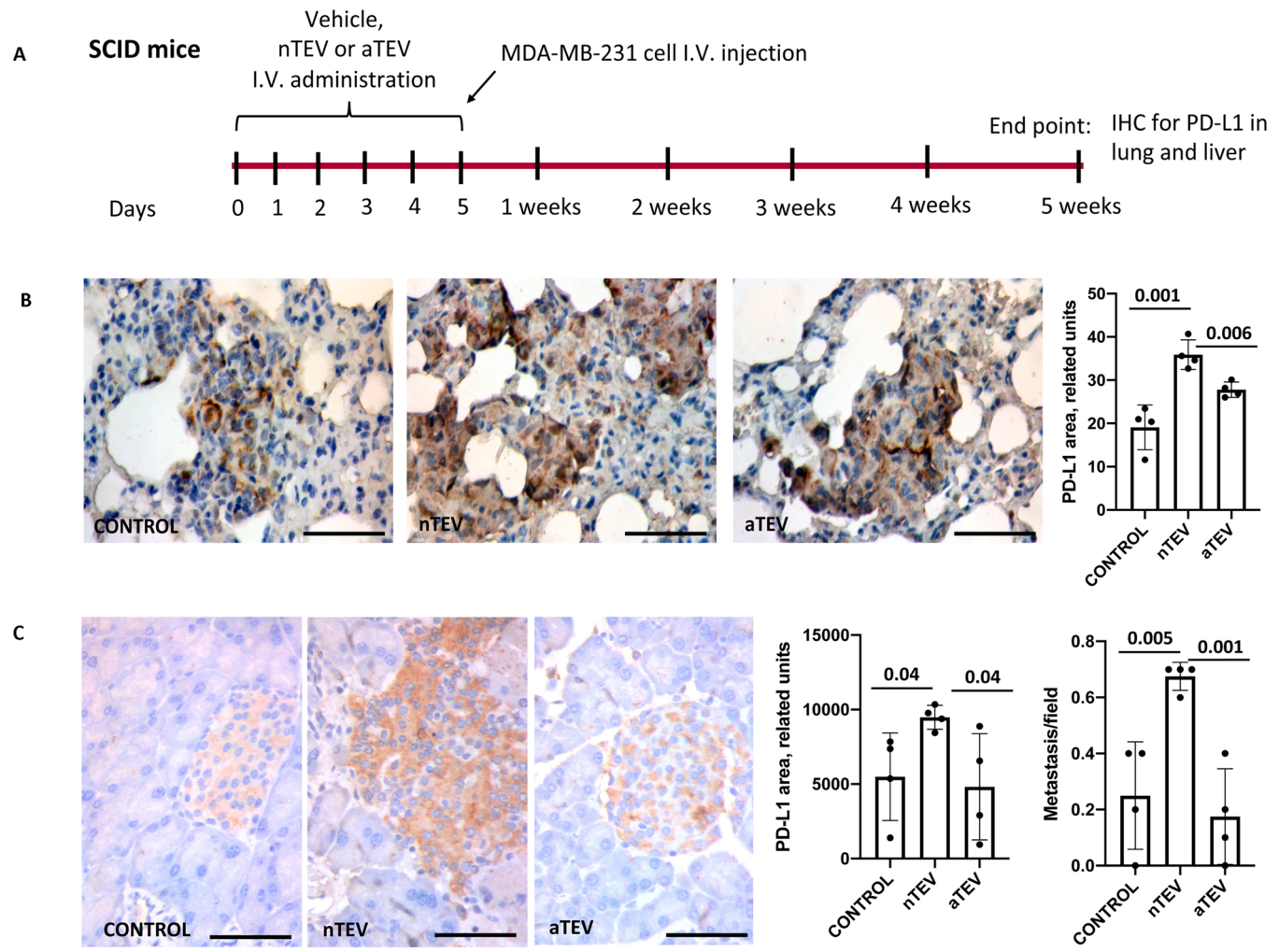


**Fig. 6.** PD-L1 expression is increased in the lung and liver tissues of SCID mice systemically primed with nTEV. (A) Schematic representation of the *in vivo* study. (B) Representative images and diagram of PD-L1 expression in lung tissues of control mice, and mice primed with nTEV or aTEV. Scale bars = 100 μm (original magnification, 400X). Diagram data are presented as the mean ± SD, n = 4. (C) Representative images of PD-L1 expression in liver tissues of control mice, and mice primed with nTEV or aTEV. Scale bars = 100 μm (original magnification, 400X). Diagram data are presented as the mean ± SD, n = 4.

bladder cancer, melanoma, and even for breast cancer [26–29]. However, the rate of success of PD-1/PD-L1 blockade in solid tumours is relatively low and mostly accompanied by both immune-related side effects [30] and TME-mediated acquired resistance [31,32]. Herein, an additional mechanism regulating PD-L1 expression in the TME is reported. In particular, we demonstrated that IL-3 signalling in TEC translates in the release of EV displaying immunosuppressive properties.

IL-3 is a hematopoietic factor mostly produced by activated T-cells, but also by monocytes/macrophages and other cell types [24]. According to proteinaltas.org (https://www.proteinatlas.org/ENSG00000185291-IL3RA/tissue) the IL-3Rα is detected in cerebral cortex and fallopian tubes in healthy subjects, while in several tumour types in cancer patients (https://www.proteinatlas.org/ENSG00000185291-IL3RA/pathology), thus suggesting the relevance of the IL-3 signalling in solid cancer. IL-3, and in particular its binding subunit, the IL-3Rα, is a well-established acute leukaemia therapeutic target, while its role in solid tumours is yet largely undetermined [33]. The observation that the IL-3Rα is highly expressed in leukaemia stem cells, compared to their normal counterpart, has provided the rational to specifically target tumour cells [22] using an anti-IL-3Rα blocking antibody [34]. In the present study, we demonstrated that a microenvironment containing IL-3 generates a positive loop involving TEC and PBMC resulting in the up regulation of the IL-3Rα in both cell types. This suggests that, as in the leukemic microenvironment, in the TME of solid tumours, the up-regulation of IL-3Rα may represent a valuable therapeutic target. Therefore, since TEC may be considered the gate for antibody entry in the TME, an antibody-based approach was used to target IL-3Rα on TEC. By means of this approach we investigated whether blocking the IL-3 signalling may "educate" TEC to rearrange the cargo of their derivatives, aTEV, thereby refining the anti-tumour immune response.

TEV are involved in key aspects of cancer growth, metastatic spread, tumour immune editing, thereby considered as relevant anti-tumour targets [2,4,35]. The regulation of TEV molecular composition is highly sensitive and specific. Protein, RNA, and lipid content changes in response to microenvironment cues. We have previously shown that blocking the IL-3 signalling in TEC led to a complex rearrangement of EV molecular composition. This results in the inhibition of their pro-oncogenic functions, according to their angiogenic and metastatic actions [3,4]. Consistent with our previous results, using TEV from tumours of different origin [2], we demonstrated that nTEV impair the anti-tumour effect of PBMC against both TEC and MDA-MB-231 cells. Notably, we demonstrated that the anti-tumour effect of PBMC was retained by aTEV-primed PBMC, indicating that IL-3Rα blockade may also act on PBMC to re-establish their cytotoxic activity. Moreover, unlike T-cells isolated after PBMC pre-conditioning naive T-cells, directly stimulated with nTEV or aTEV, have no effect on tumour cells. This observation strongly supports the notion that nTEV-mediated immune regulation mainly involves mechanisms orchestrated by

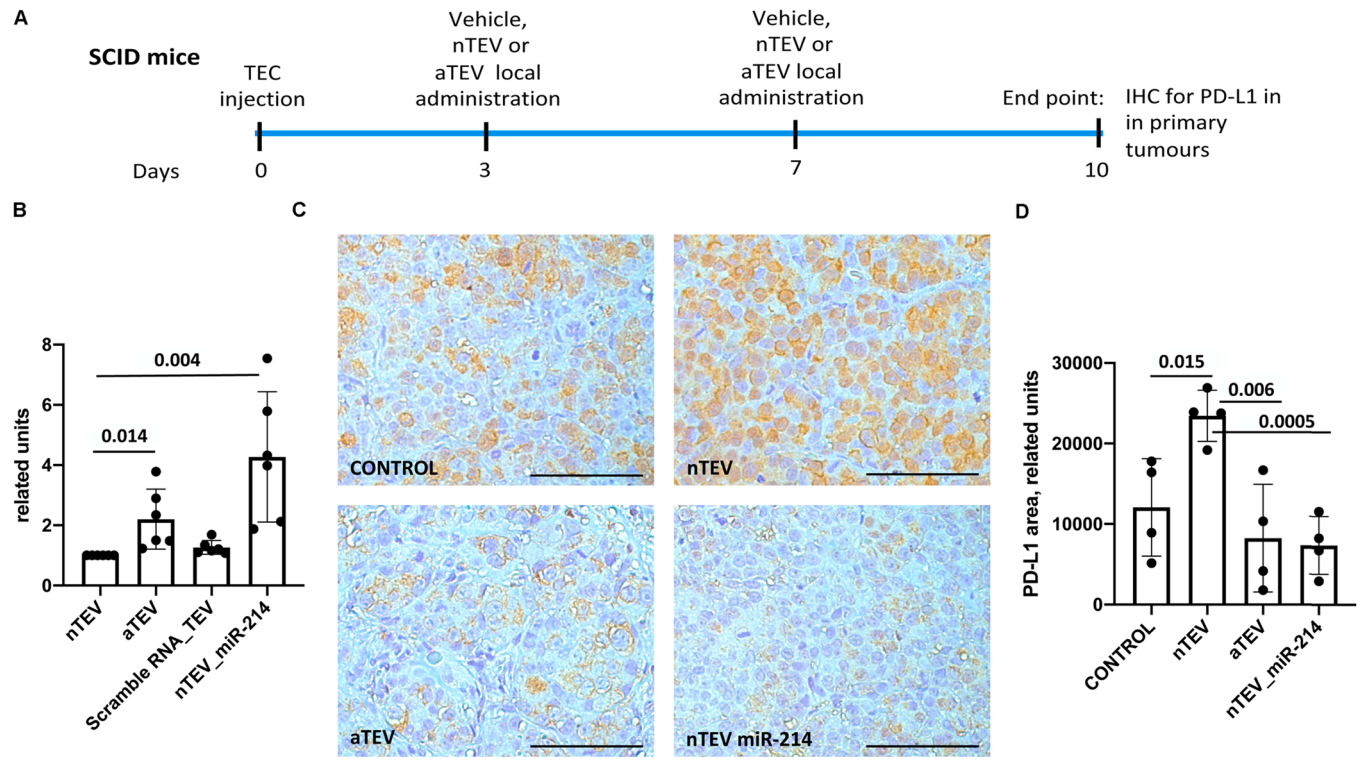


**Fig. 7.** miR-214 controls PD-L1 expression in *vivo*. (A) Schematic representation of the *in vivo* study. (B) Diagram of PCR analysis of miR-214 expression in nTEV, aTEV and nTEV_miR-214. As a control Scramble RNA was used. Data are presented as the mean ± SD, n = 6. Representative images (C) and diagram (D) of PD-L1 staining on TEC in control tumours, and in tumours from mice locally treated with nTEV, aTEV or nTEV_miR-214. Scale bars = 100 μm (original magnification, 400X). Diagram data are presented as the mean ± SD, n = 4.

antigen-presenting cells. As a matter of fact, we demonstrated that nTEV, but not aTEV, increased the expression of PD-L1 on primary myeloid cells *in vitro* and *in vivo* in an immunocompetent model. This observation provides the first evidence that nTEV can control PD-L1 expression in an immunocompetent context.

PD-L1 is expressed by different tumour cell types [36], and its overexpression represents one of the most relevant mechanisms of T-cell exhaustion [37] and tumour progression. We herein demonstrated that intra-tumour nTEV injections was able to increase the expression of PD-L1 on tumour cells, and, more importantly, that aTEV bring back PD-L1 expression to the control level. Using a different mouse model, we also demonstrated that nTEV and aTEV can differently modulate PD-L1 expression in tumour cells engaged into metastatic sites. Of note, in this model we found that the expression of PD-L1 correlated with the number of metastases both in the lung and in the liver. Therefore, these results demonstrate that an antibody-based approach against the IL-3Rα may reshape PD-L1 expression and the anti-tumour immune response, *via* aTEV.

Different mechanisms control PD-L1 expression in cancer [38]. Inflammatory cytokines released in the TME have been reported to boost the expression of PD-L1 in tumour and stromal cells [39,40]. We herein demonstrated that the inflammatory cytokine IL-3, released in the TME, besides controlling the tumour vasculature takes part in cancer immune escape, *via* nTEV. Moreover, the observation that IL-10 was increased when PBMC were primed with nTEV and left in co-cultures with cancer cells, sustains the role of nTEV in the reshuffle of the TME secretome and in tumour immune suppression. The ability of aTEV to reverse PBMC secretome and to re-establish PBMC-mediated anti-tumour cytotoxic activity, further supports the role of IL-3 in tumour immune tolerance.

Several studies have designated EV as PD-L1 delivery system [10]. However, we failed to detect PD-L1 in nTEV suggesting that, rather than transferring PD-L1 to immune or tumour cells, nTEV tune the adaptive immune response by a mechanism involving their cargo.

Epigenetic mechanisms such as histone acetylation/methylation or abnormal miRNA expression are instrumental for cancer immune escape *via* PD-L1 expression [25,38]. miR-200, miR-326, miR-34a and miR-214 are from among the most relevant miRNAs involved in PD-L1 expression [25,38,42]. Consistent with these data, we demonstrated that the enrichment of miR-214 in aTEV down-regulates PD-L1 expression and may conceivably break down tumour immune evasion. However, since EV action rely on their entire cargo we cannot rule out the possibility that cancer microenvironment can hijack the TEV cargo at different level to facilitate discrete mechanisms of the multi-step cancer process.

## 5. Conclusions

Overall, we provide evidence that interfering with the IL-3 signalling, by blocking the activity of its receptor at the entrance of the TME, may be instrumental for reschedule the anti-tumour immune response. Downregulating PD-L1 expression in myeloid cells also improves the response of combined immune checkpoint approaches [43]. Therefore, our findings offer a new therapeutic window to boost and reshape the aberrant immune response in solid tumour.

## CRediT authorship contribution statement

TL was involved in conceptualization, methodology, data curation and writing the original draft; MK provided formal analysis of *in vitro* and *in vivo* experiments; CG performed *in vitro* and *in vivo* experiments and provided formal analysis of the *in vitro* and *in vivo* studies; MC performed the animal studies; SF isolated and characterized extracellular vesicles; GL performed the animal study; EF performed *in vitro* studies; MFB was involved in conceptualization, supervision, writing, review and editing the Ms, as well as in providing resources.

## Declaration of Competing Interest

The authors declare no conflict of interest.

## Acknowledgements

The authors acknowledge the technical support of Dr. Federica Antico, Prof. Stefania Bruno, and Dr. Chiara Gai. A special thanks to Prof. Giovanni Camussi and Dr. Chiara Deregibus for TEM analysis.

*Sources of funding*

This work has been supported by grants obtained by MFB from Ministero dell'Istruzione, Ministero Italiano Università Ricerca (MIUR), Italy ex 60%.

## Appendix A. Supporting information

Supplementary data associated with this article can be found in the online version at doi:10.1016/j.phrs.2022.106206.

## References

[1] T.L. Whiteside, Exosomes and tumor-mediated immune suppression, J. Clin. Invest. vol. 126 (4) (. 2016) 1216–1223, https://doi.org/10.1172/JCI81136.
[2] T. Lopatina, et al., Extracellular vesicles released by tumor endothelial cells spread immunosuppressive and transforming signals through various recipient cells, Front. Cell Dev. Biol. vol. 8 (2020), https://doi.org/10.3389/fcell.2020.00698.
[3] G. Lombardo, et al., IL-3R-alpha blockade inhibits tumor endothelial cell-derived extracellular vesicle (EV)-mediated vessel formation by targeting the β-catenin pathway, Oncogene vol. 37 (9) (. 2018) 1175–1191, https://doi.org/10.1038/s41388-017-0034-x.
[4] T. Lopatina, et al., Targeting IL-3Rα on tumor-derived endothelial cells blunts metastatic spread of triple-negative breast cancer via extracellular vesicle reprogramming, Oncogenesis vol. 9 (10) (10, . 2020), https://doi.org/10.1038/s41389-020-00274-y.
[5] "A miRNA signature in endothelial cell-derived extracellular vesicles in tumor-bearing mice | Scientific Reports."https://www.nature.com/articles/s41598–019-52466–1 (Accessed 22 December 2021).
[6] K. Taguchi, T. Onoe, T. Yoshida, Y. Yamashita, Y. Tanaka, H. Ohdan, Tumor Endothelial Cell-Mediated Antigen-Specific T-cell Suppression via the PD-1/PD-L1 Pathway, Mol. Cancer Res. MCR vol. 18 (9) (. 2020) 1427–1440, https://doi.org/10.1158/1541-7786.MCR-19-0897.
[7] Y. Han, D. Liu, L. Li, PD-1/PD-L1 pathway: current researches in cancer, Am. J. Cancer Res. vol. 10 (3) (. 2020) 727–742.
[8] A.H. Sharpe, K.E. Pauken, The diverse functions of the PD1 inhibitory pathway, Nat. Rev. Immunol. vol. 18 (3) (. 2018) 153–167, https://doi.org/10.1038/nri.2017.108.
[9] V.R. Juneja, et al., PD-L1 on tumor cells is sufficient for immune evasion in immunogenic tumors and inhibits CD8 T cell cytotoxicity, J. Exp. Med. vol. 214 (4) (. 2017) 895–904, https://doi.org/10.1084/jem.20160801.
[10] G. Chen, et al., Exosomal PD-L1 contributes to immunosuppression and is associated with anti-PD-1 response, Nature vol. 560 (7718) (. 2018) 382–386, https://doi.org/10.1038/s41586-018-0392-8.
[11] M. Poggio, et al., Suppression of exosomal PD-L1 induces systemic anti-tumor immunity and memory, e13, Cell vol. 177 (2) (. 2019) 414–427, https://doi.org/10.1016/j.cell.2019.02.016.
[12] F.L. Ricklefs, et al., Immune evasion mediated by PD-L1 on glioblastoma-derived extracellular vesicles, eaar2766, Sci. Adv. vol. 4 (3) (. 2018), https://doi.org/10.1126/sciadv.aar2766.
[13] M.J. Cox, et al., Leukemic extracellular vesicles induce chimeric antigen receptor T cell dysfunction in chronic lymphocytic leukemia, Mol. Ther. J. Am. Soc. Gene Ther. vol. 29 (4) (. 2021) 1529–1540, https://doi.org/10.1016/j.ymthe.2020.12.033.
[14] J. Zhou, et al., Soluble PD-L1 as a biomarker in malignant melanoma treated with checkpoint blockade, Cancer Immunol. Res. vol. 5 (6) (. 2017) 480–492, https://doi.org/10.1158/2326-6066.CIR-16-0329.
[15] M.-N. Theodoraki, S.S. Yerneni, T.K. Hoffmann, W.E. Gooding, T.L. Whiteside, Clinical significance of pd-l1+ exosomes in plasma of head and neck cancer patients, J. Am. Assoc. Cancer Res. vol. 24 (4) (. 2018) 896–905, https://doi.org/10.1158/1078-0432.CCR-17-2664.
[16] S. Ludwig, et al., Suppression of lymphocyte functions by plasma exosomes correlates with disease activity in patients with head and neck cancer, Clin. Cancer Res. . J. Am. Assoc. Cancer Res. vol. 23 (16) (. 2017) 4843–4854, https://doi.org/10.1158/1078-0432.CCR-16-2819.
[17] D.A.-M. Annan, H. Kikuchi, N. Maishi, Y. Hida, K. Hida, Tumor endothelial cell—a biological tool for translational cancer research, Int. J. Mol. Sci. vol. 21 (9) (. 2020), https://doi.org/10.3390/ijms21093238.
[18] H. Ohmura-Kakutani, et al., Identification of tumor endothelial cells with high aldehyde dehydrogenase activity and a highly angiogenic phenotype, PLOS ONE vol. 9 (12) (. 2014), e113910, https://doi.org/10.1371/journal.pone.0113910.
[19] B. Bussolati, I. Deambrosis, S. Russo, M.C. Deregibus, G. Camussi, Altered angiogenesis and survival in human tumor-derived endothelial cells, FASEB J. vol. 17 (9) (2003) 1159–1161, https://doi.org/10.1096/fj.02-0557fje.
[20] D. Lambrechts, et al., Phenotype molding of stromal cells in the lung tumor microenvironment, Nat. Med. vol. 24 (8) (. 2018) 1277–1289, https://doi.org/10.1038/s41591-018-0096-5.
[21] P. Dentelli, A. Rosso, C. Olgasi, G. Camussi, M.F. Brizzi, IL-3 is a novel target to interfere with tumor vasculature, Oncogene vol. 30 (50) (. 2011) 4930–4940, https://doi.org/10.1038/onc.2011.204.
[22] I. Aldoss, M. Clark, J.Y. Song, V. Pullarkat, Targeting the alpha subunit of IL-3 receptor (CD123) in patients with acute leukemia, Hum. Vaccin. Immunother. vol. 16 (10) (. 2020) 2341–2348, https://doi.org/10.1080/21645515.2020.1788299.
[23] T. Lopatina, et al., Extracellular vesicles from human liver stem cells inhibit a angiogenesis, Int. J. Cancer vol. 144 (2) (. 2019) 322–333, https://doi.org/10.1002/ijc.31796.
[24] M.C. Deregibus, et al., Charge-based precipitation of extracellular vesicles,", Int. J. Mol. Med. vol. 38 (5) (. 2016) 1359–1366, https://doi.org/10.3892/ijmm.2016.2759.
[25] S.E. Broughton, et al., The GM-CSF/IL-3/IL-5 cytokine receptor family: from ligand recognition to initiation of signaling, Immunol. Rev. vol. 250 (1) (. 2012) 277–302, https://doi.org/10.1111/j.1600-065X.2012.01164.x.
[26] J.-R. Sun, X. Zhang, Y. Zhang, MiR-214 prevents the progression of diffuse large B-cell lymphoma by targeting PD-L1, Cell. Mol. Biol. Lett. vol. 24 (1) (. 2019) 68, https://doi.org/10.1186/s11658-019-0190-9.
[27] "Pembrolizumab versus Chemotherapy for PD-L1–Positive Non–Small-Cell Lung Cancer | NEJM." https://www.nejm.org/doi/full/10.1056/nejmoa1606774 (Accessed 22 December 2021).
[28] "Nivolumab versus Everolimus in Advanced Renal-Cell Carcinoma | NEJM." https://www.nejm.org/doi/full/10.1056/nejmoa1510665 (Accessed 22 December 2021).
[29] "Pembrolizumab as Second-Line Therapy for Advanced Urothelial Carcinoma | NEJM." https://www.nejm.org/doi/full/10.1056/nejmoa1613683 (Accessed 22 December 2021).
[30] P. Schmid, et al., Atezolizumab and Nab-Paclitaxel in Advanced Triple-Negative Breast Cancer, N. Engl. J. Med. vol. 379 (22) (. 2018) 2108–2121, https://doi.org/10.1056/NEJMoa1809615.
[31] F. Martins, et al., Adverse effects of immune-checkpoint inhibitors: epidemiology, management and surveillance, Nat. Rev. Clin. Oncol. vol. 16 (9) (. 2019) 563–580, https://doi.org/10.1038/s41571-019-0218-0.
[32] R. Pathak, R.R. Pharaon, A. Mohanty, V.M. Villaflor, R. Salgia, E. Massarelli, Acquired resistance to PD-1/PD-L1 blockade in lung cancer: mechanisms and patterns of failure, Cancers vol. 12 (12) (. 2020) 3851, https://doi.org/10.3390/cancers12123851.
[33] Y. Shi. et al. Acquired resistance to PD-L1 inhibition is associated with an enhanced type I IFN-stimulated secretory program in tumor cells 2021.
[34] U. Testa, R. Riccioni, D. Diverio, A. Rossini, F. Lo Coco, C. Peschle, Interleukin-3 receptor in acute leukemia, Leukemia vol. 18 (2) (. 2004) 219–226, https://doi.org/10.1038/sj.leu.2403224.
[35] "Full article: A Phase 1 study of the safety, pharmacokinetics and anti-leukemic activity of the anti-CD123 monoclonal antibody CSL360 in relapsed, refractory or high-risk acute myeloid leukemia." https://www.tandfonline.com/doi/full/10.3109/10428194.2014.956316 (Accessed 22 December 2021).
[36] R. Kalluri, The biology and function of exosomes in cancer, J. Clin. Invest. vol. 126 (4) (. 2016) 1208–1215, https://doi.org/10.1172/JCI81135.
[37] A.H. Sharpe, E.J. Wherry, R. Ahmed, G.J. Freeman, The function of programmed cell death 1 and its ligands in regulating autoimmunity and infection, Nat. Immunol. vol. 8 (3) (. 2007) 239–245, https://doi.org/10.1038/ni1443.
[38] K.E. Pauken, E.J. Wherry, Overcoming T cell exhaustion in infection and cancer, Trends Immunol. vol. 36 (4) (. 2015) 265–276, https://doi.org/10.1016/j.it.2015.02.008.
[39] J.-H. Cha, L.-C. Chan, C.-W. Li, J.L. Hsu, M.-C. Hung, Mechanisms Controlling PD-L1 Expression in Cancer, Mol. Cell vol. 76 (3) (. 2019) 359–370, https://doi.org/10.1016/j.molcel.2019.09.030.
[40] X. Wang, et al., Inflammatory cytokines IL-17 and TNF-α up-regulate PD-L1 expression in human prostate and colon cancer cells, Immunol. Lett. vol. 184 (. 2017) 7–14, https://doi.org/10.1016/j.imlet.2017.02.006.
[42] L. Shao, et al., MicroRNA-326 attenuates immune escape and prevents metastasis in lung adenocarcinoma by targeting PD-L1 and B7-H3, Cell Death Disco vol. 7 (1) (. 2021) 1–10, https://doi.org/10.1038/s41420-021-00527-8.
[43] E. Anastasiadou, et al., MiR-200c-3p Contrasts PD-L1 induction by combinatorial therapies and slows proliferation of epithelial ovarian cancer through downregulation of β-catenin and c-myc, Cells vol. 10 (3) (. 2021) 519, https://doi.org/10.3390/cells10030519.